

Supplementary Material for

Cerebellar heterogeneity and its impact on PET data quantification of 5-HT receptor radioligands

Melanie Ganz¹, Ling Feng¹, Hanne Demant Hansen¹, Vincent Beliveau^{1,2}, Claus Svarer¹, Gitte M. Knudsen^{1,2}, Douglas N. Greve^{3,4}

¹Neurobiology Research Unit and Center for Integrated Molecular Brain Imaging, Rigshospitalet, Copenhagen, Denmark

²Faculty of Health and Medical Sciences, University of Copenhagen, Copenhagen, Denmark

³Athinoula A. Martinos Center for Biomedical Imaging, Department of Radiology, Massachusetts General Hospital, Boston, MA, USA

⁴Harvard Medical School, Boston, MA, USA

Corresponding author:

Gitte Moos Knudsen, Neurobiology Research Unit, 28 Juliane Maries Vej, Rigshospitalet, building 6931, 2100 Copenhagen, Denmark.

1 Demographic information

Radioligand	[¹¹ C]DASB	[¹¹ C]CUMI-101	[¹¹ C]AZ10419369	[¹¹ C]Cimbi-36	[¹¹ C]SB207145
N	100	8	36	29	59
Gender (M/F)	29/71	3/5	24/12	15/14	41/18
Age (mean±std)	25.1±5.8	28.4±8.8	27.8±6.9	22.6±2.7	25.9±5.3
Age (min-max)	18.4-44.9	20.1-43.9	18.8-44.8	18.4-28.7	20.1-44.8
BMI (kg/m²) (mean±std)	23.2±2.9	22.7±2.6	24.9±4.3	23.4±2.4	23.5±3.3
Injected Dose (MBq) (mean±std)	586.0±32.2	510.5±149.1	585.4±37.4	510.4±109.7	577.1±70.9
Injected Mass (µg) (mean±std)	1.9±2.2	2.0±1.5	1.2±1.0	0.8±0.5	1.1±0.7

Table 1. Demographic details of the included healthy subjects.

2 PET scanning parameters

Radioligand	[¹¹ C]DASB	[¹¹ C]CUMI-101	[¹¹ C]AZ10419369	[¹¹ C]Cimbi-36	[¹¹ C]SB207145
Scan time (min)	90	120	90	120	120
Frame lengths (number x sec)	6x10, 3x20, 6x30, 5x60, 5x120, 8x300, 3x600	6x5, 10x15, 4x30, 5x120, 5x300, 8x600	6x10, 6x20, 6x60, 8x120, 19x300	6x10, 6x20, 6x60, 8x120, 19x300	6x5, 10x15, 4x30, 5x120, 5x300, 8x600
Realigned frames (first:last)	10:36	10:38	13:45	13:45	10:38
Reference frame	26	26	27	27	26

Table 2. Details of the PET scanning parameters as well as the realignment procedure.

3 MR scanning parameters

The acquisition parameters for the four MR scanners were the following:

- Siemens Verio: sagittal, magnetization prepared rapid gradient echo (MPRAGE) scan of the head: echo time (TE)/repetition time (TR)/ inversion time (TI) = 2.32/1900/900 ms; slice resolution=100%; bandwidth=200 (Hz/Px); echo spacing=7.1 ms; flip angle= 9°; field of view (FOV)=230 mm; matrix 256x256 (base resolution); (slices/slab: 224); GRAPPA acceleration factor 2; 0.9x0.9x0.9mm voxels; 224 slices, acquisition time = 8.50 minutes.
- Siemens Trio: sagittal, magnetization prepared rapid gradient echo (MPRAGE) scan of the head: echo time (TE)/repetition time (TR)/ inversion time (TI) = 3.04/1550/800 ms; slice resolution=100%; bandwidth=170 (Hz/Px); echo spacing=7.7 ms; flip angle=9°; field of view (FOV)=256 mm; matrix 256x256; 1x1x1mm voxels; 192 slices, acquisition time = 6.32 minutes.
- Siemens Prisma: sagittal, magnetization prepared rapid gradient echo (MPRAGE) scan of the head: echo time (TE)/repetition time (TR)/ inversion time (TI) = 2.58/1900/900 ms; slice resolution= 100 %; bandwidth= 170 (Hz/Px); echo spacing= 7.8 ms; flip angle= 9°; field of view (FOV)=230 mm; matrix 256x256 (base resolution); (slices/slab: 224); GRAPPA acceleration factor 2; 0.9x0.9x0.9mm voxels; 224 slices, acquisition time = 4.26 minutes.

4 Overview of differences in cerebellar uptake and neocortical binding potential

Difference in MeanSUV	CH vs. CV	CH vs. CW	CH vs. Total Cb	CV vs. CW	CV vs. Total Cb	CW vs. Total Cb
[¹¹ C]CUMI	0.0094	0.0094	0.0094	0.0094	0.0094	0.0094
[¹¹ C]AZ10419369	0.0017	0.0014	0.0011	0.1357	0.0058	0.0014
[¹¹ C]Cimbi-36	0.0001	0.0000	0.0000	0.0000	0.0000	0.0000
[¹¹ C]SB207145	0.2366	0.0000	0.0000	0.0000	0.0000	0.0000
[¹¹ C]DASB	0.0000	0.0000	0.0000	0.0781	0.0000	0.0000

(a)

Difference in neocortical BP _{ND}	CH vs. CV	CH vs. CW	CH vs. Total Cb	CV vs. CW	CV vs. Total Cb	CW vs. Total Cb
[¹¹ C]CUMI	0.0094	0.0094	0.0094	0.0094	0.0094	0.0094
[¹¹ C]AZ10419369	0.0000	0.3792	0.1219	0.0011	0.0000	0.4761
[¹¹ C]Cimbi-36	0.4904	0.0000	0.0000	0.0000	0.4265	0.0000
[¹¹ C]SB207145	0.2542	0.0000	0.0000	0.0000	0.5611	0.0000
[¹¹ C]DASB	0.0000	d.n.a.	0.0000	d.n.a.	0.0000	d.n.a.

(b)

Table 3. Overview of differences in cerebellar uptake and neocortical binding potential based on different reference region definitions. (a) Outcome of within subjects, paired nonparametric two-sided Wilcoxon signed rank tests between mean SUV in all regions. (b) Outcome of within subjects, paired nonparametric two-sided Wilcoxon signed rank tests between neocortical BP_{ND} based on the different regions. All p-values were globally (over mean SUV and BP_{ND}) corrected for FDR<0.05¹.

5 Neocortical binding potential using CH, CV, and CW as reference region

Tracer	Mean BP _{nd} CH	Std BP _{nd} CH	Mean BP _{nd} CV	Std BP _{nd} CV	Mean BP _{nd} CW	Std BP _{nd} CW	Mean BP _{nd} Total Cb	Std BP _{nd} Total Cb
[¹¹ C]CUMI-101	1.58	0.27	1.38	0.29	2.33	0.37	1.69	0.28
[¹¹ C]AZ10419369	1.56	0.25	1.69	0.31	1.6	0.26	1.57	0.24
[¹¹ C]Cimbi-36	1.51	0.18	1.49	0.19	1.33	0.14	1.47	0.17
[¹¹ C]SB207145	0.79	0.08	0.8	0.1	0.85	0.1	0.8	0.08
[¹¹ C]DASB	0.48	0.08	0.33	0.08	d.n.f.	d.n.f.	0.42	0.07

Table 4. Mean and standard deviation of neocortical binding potential values using CH, CV CW and total Cb as reference region, respectively (d.n.f.: does not fit).

6 Blocking experiments

A. [¹¹C]CUMI-101 blocking experiments

One of the [¹¹C]CUMI-101 subjects underwent a pindolol blocking scan. Orally pindolol administration started three days before scanning: 3 times per day (2.5mgx3 on day one, 5mgx3 2nd day, and 7.5mgx3 3rd day), 7.5mg in the morning of scanning, and 7.5mg one hour before scanning. The distribution volumes (V_T) of both the baseline scan and the blocking scan were quantified using a 2 tissue compartment model with 4 parameters. Based on an occupancy plot of 23 ROIs and cerebellum before and after pindolol injection we calculate the occupancy to be around 48% and $V_{ND}=3.7$. In order to derive this we used the relationship between baseline and blocking V_T of the form: $V_{T,block} = (1 - O) \cdot V_{T,base} + O \cdot V_{T,base}$

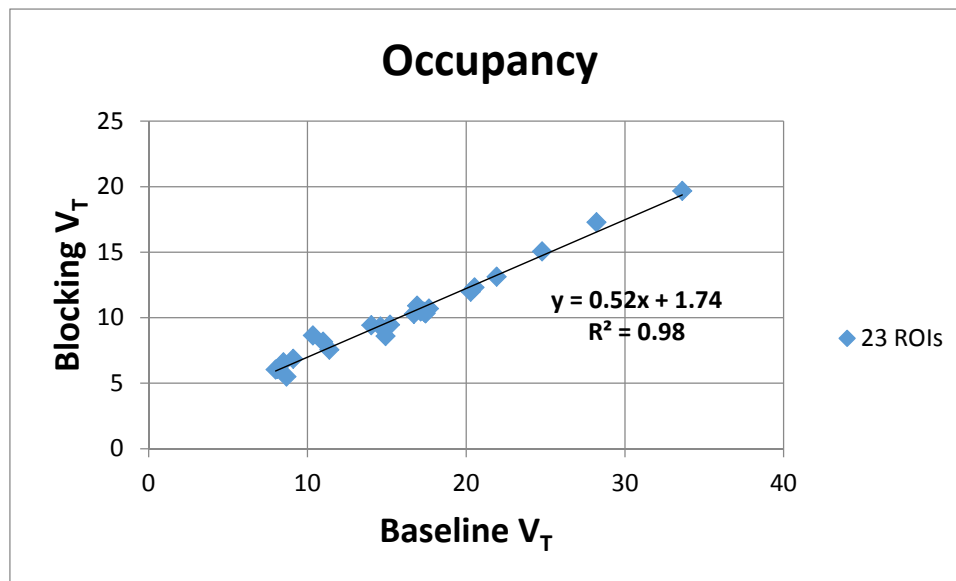


Figure 1. Occupancy plot of the effect of pindolol on [¹¹C]CUMI-101 binding.

Calculating the difference between the baseline V_T and the derived V_{ND} yields the smallest difference for CW and total cerebellum (which is largely driven by CW) and thereafter CH, CH+CV and finally CV.

Distribution volume (mL cm ⁻³)	CH	CV	CH+CV	CW	Total cb
Baseline V _T	7.68	8.87	7.85	5.86	7.41
Baseline V _T - V _{ND}	4.01	5.21	4.18	2.20	3.74

Table 5. Baseline V_T and difference to V_{ND} estimated for the single [¹¹C]CUMI blocking subject.

From the shape of the baseline and blocking SUVs displayed in Figure 2 we can deduce two things: 1) The kinetics of all reference regions, CW, CH, CV and CH+CV is similar. 2) Furthermore, blocking should bring receptor-rich region closer to receptor-free regions and we see an effect of this exhibit itself in the case of CV.

[¹¹C]CUMI-101 Baseline and blocking data

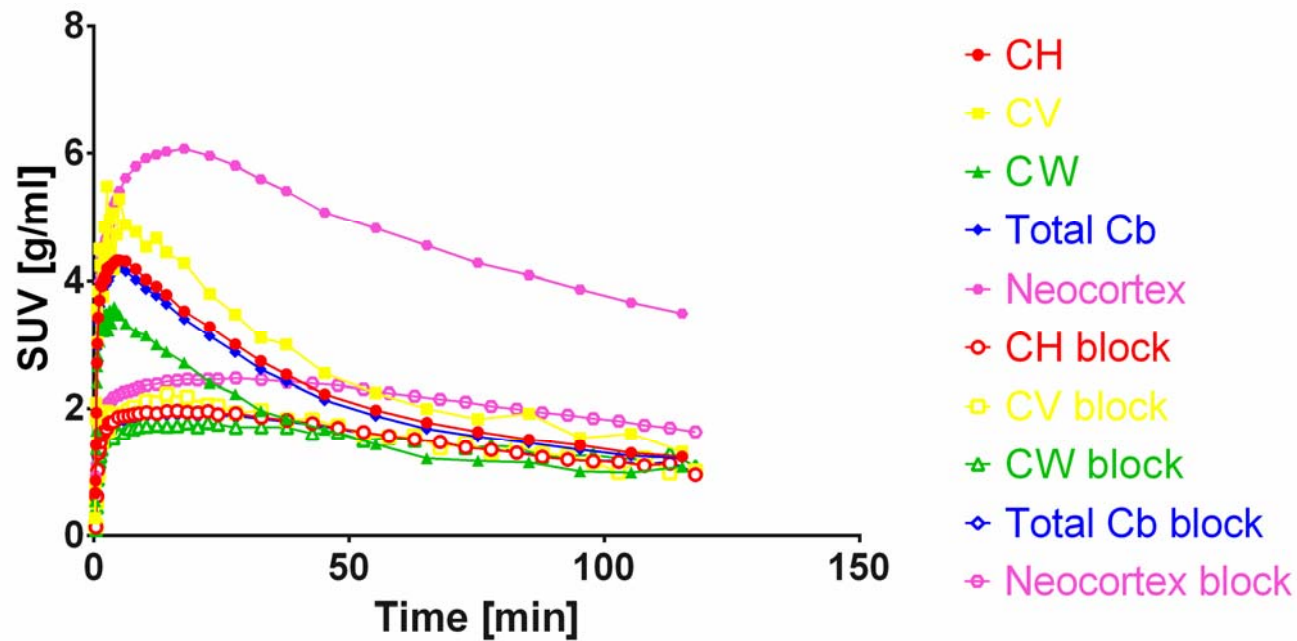


Figure 2. Baseline and blocking SUVs for the [¹¹C]CUMI-101 blocking subject.

B. [¹¹C]Cimbi-36 blocking experiments

Based on four Cimbi-36 subjects (we needed to exclude Subject 5 since not all of cerebellum was covered in the PET scan), we can derive the V_T for five different reference regions, CH, CV, CH+CV as well as additionally requested in a comment below cerebellar white matter (CW) and total cerebellum using arterial input and a 2 tissue compartment model². We can compare the V_T of the five reference regions to the true non-displaceable binding derived in the associated blocking studies and presented in Table 2 of Ettrup et al.². Calculating the sum of squared differences (SSD) between the V_{ND} and the V_T of the different reference regions, we find that CH is the reference region that most closely relates to V_{ND} derived from blocking experiments, followed by using CH+CV, the whole cerebellum, CW and finally CV. The reason that CH+CV ranks high is that CV has a small influence on the arterial modeling of the whole region CH+CV. Also CW is besides CV performing the worst.

Baseline V_T	CH	CV	CH+CV	CW	Total cb
Subject 1	10.19	10.20	10.02	10.08	9.96
Subject 2	11.36	9.10	11.20	11.36	11.40
Subject 3	10.37	10.43	10.38	10.70	10.43
Subject 4	13.51	14.32	13.56	14.23	13.68

(a)

V_{ND} - Baseline V_T	CH	CV	CH+CV	CW	Total cb
Subject 1	2.41	2.40	2.58	2.52	2.64
Subject 2	1.34	3.60	1.50	1.34	1.30
Subject 3	1.33	1.27	1.32	1.00	1.27
Subject 4	-1.61	-2.42	-1.66	-2.33	-1.78
SSD	11.97	26.14	13.40	14.59	13.45

(b)

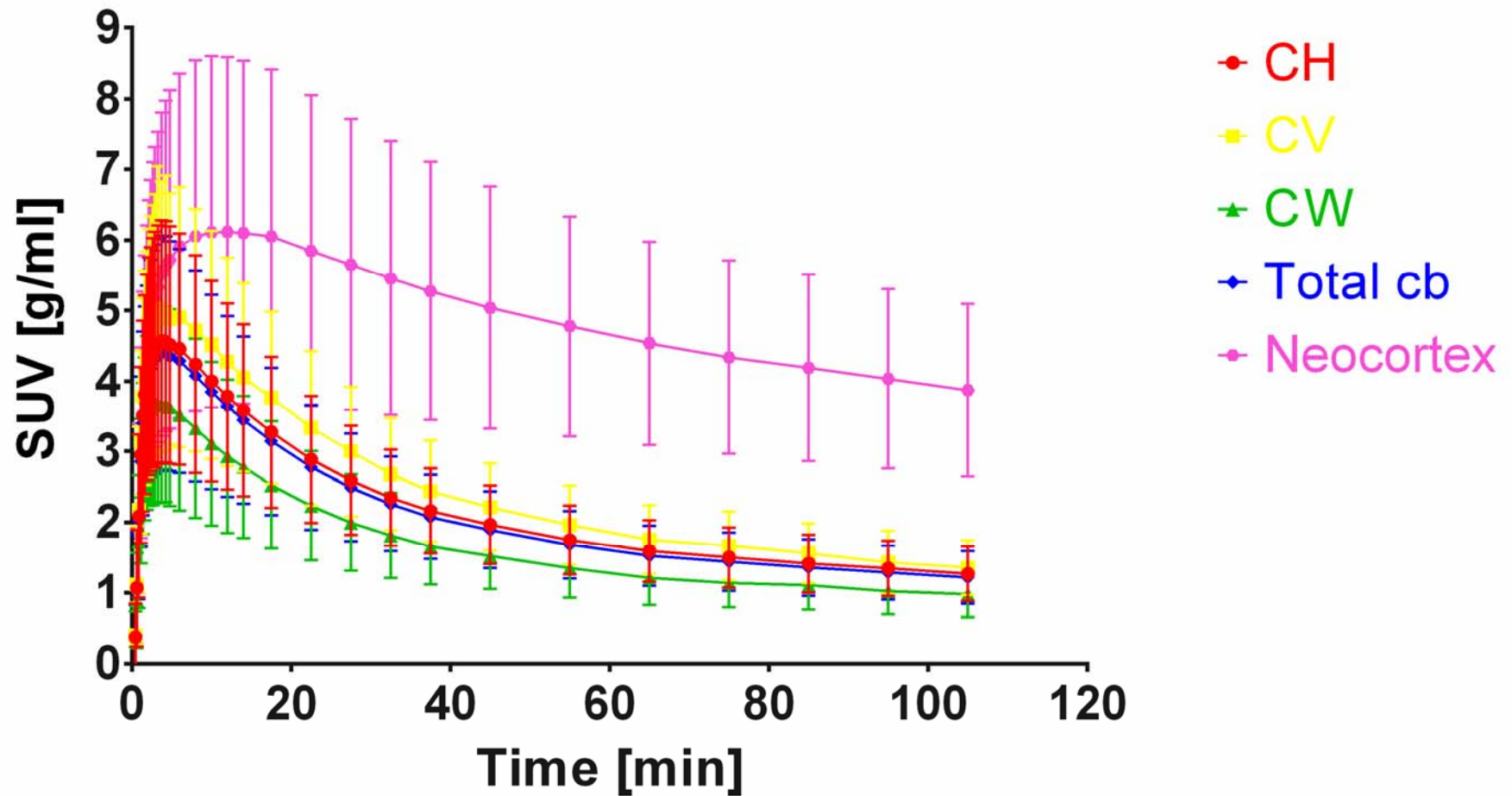
Table 6. (a) Baseline V_T and (b) difference to V_{ND} estimated from blocking for four subjects from Ettrup et al.²

7 Mean SUV curves

In the following we show standardized uptake value (SUV) curves for all ligands for all regions of interest in cerebellum (CH, CV, CH+CV, CW, total cerebellum) as well as neocortex as mean+SD curves. The curves already show the differences we observe between the different regions.

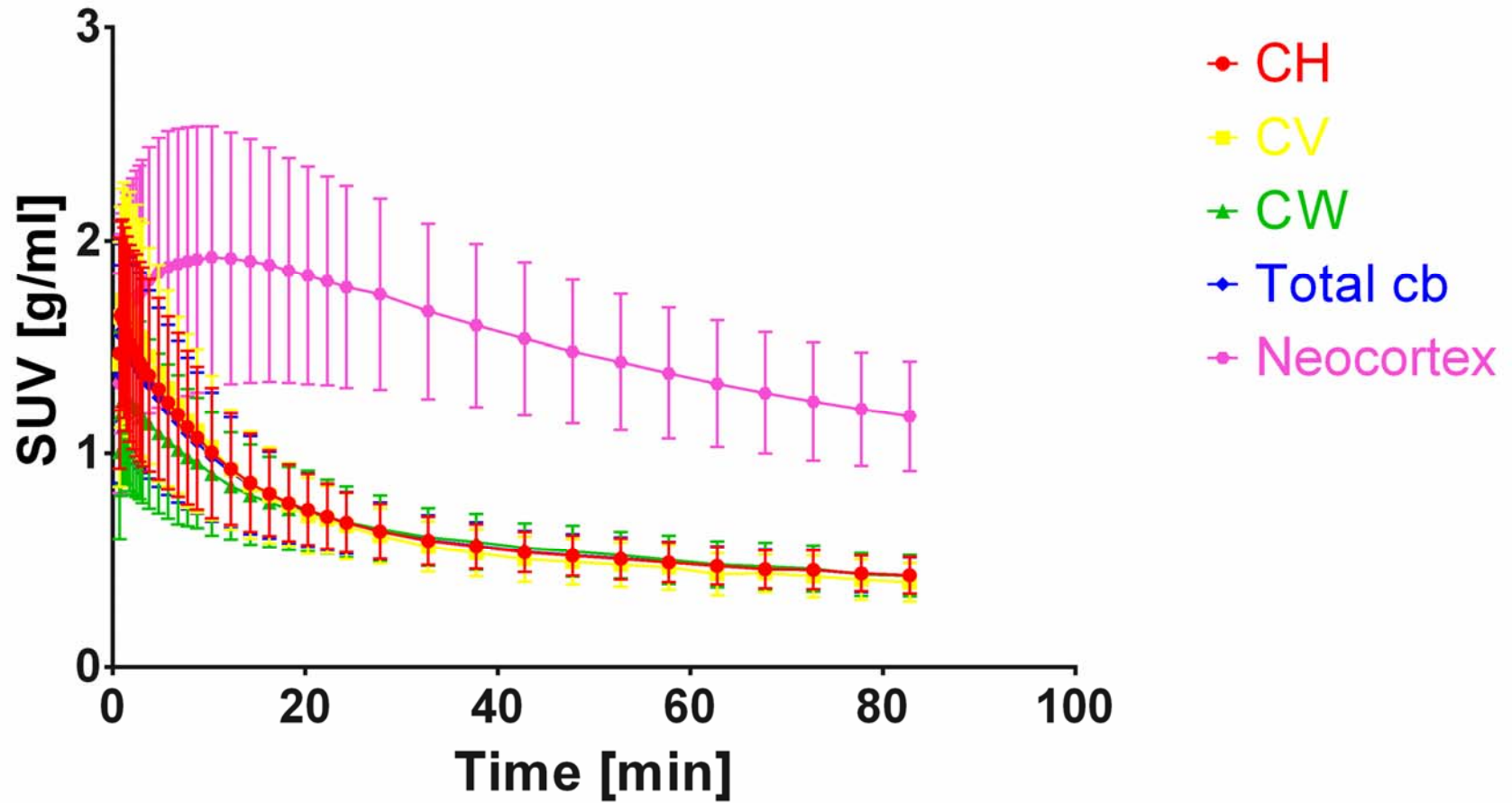
For [11C]CUMI-101 the neocortex SUV is as expected the highest followed by the vermis SUV. Next, the SUVs of total cerebellum, CH+CV and CH lie very close to each other and finally the SUV of CW is lowest. The kinetics are very similar for all reference regions. Regarding the SUVs for [11C]AZ10419369 there is almost no difference between the SUVs of CV, CH, CH+CV and total cerebellum, while CW again has slightly slower kinetics. While the ordering of the SUVs is again similar for the case of [11C]Cimbi-36, the average SUVs here highlight the different and slower kinetics of CW compared with CV, CH, CH+CV and the total cerebellum. In the case of [11C]SB207145 we observe the same difference in kinetics between CV, CH, CH+CV and CW albeit the difference is smaller than in the case of [11C]Cimbi-36. Finally, the average SUVs for [11C]DASB have again the same ranking, but additionally show a time shift in the white matter kinetics.

Mean SUV curves for [^{11}C]CUMI-101 (n=8)



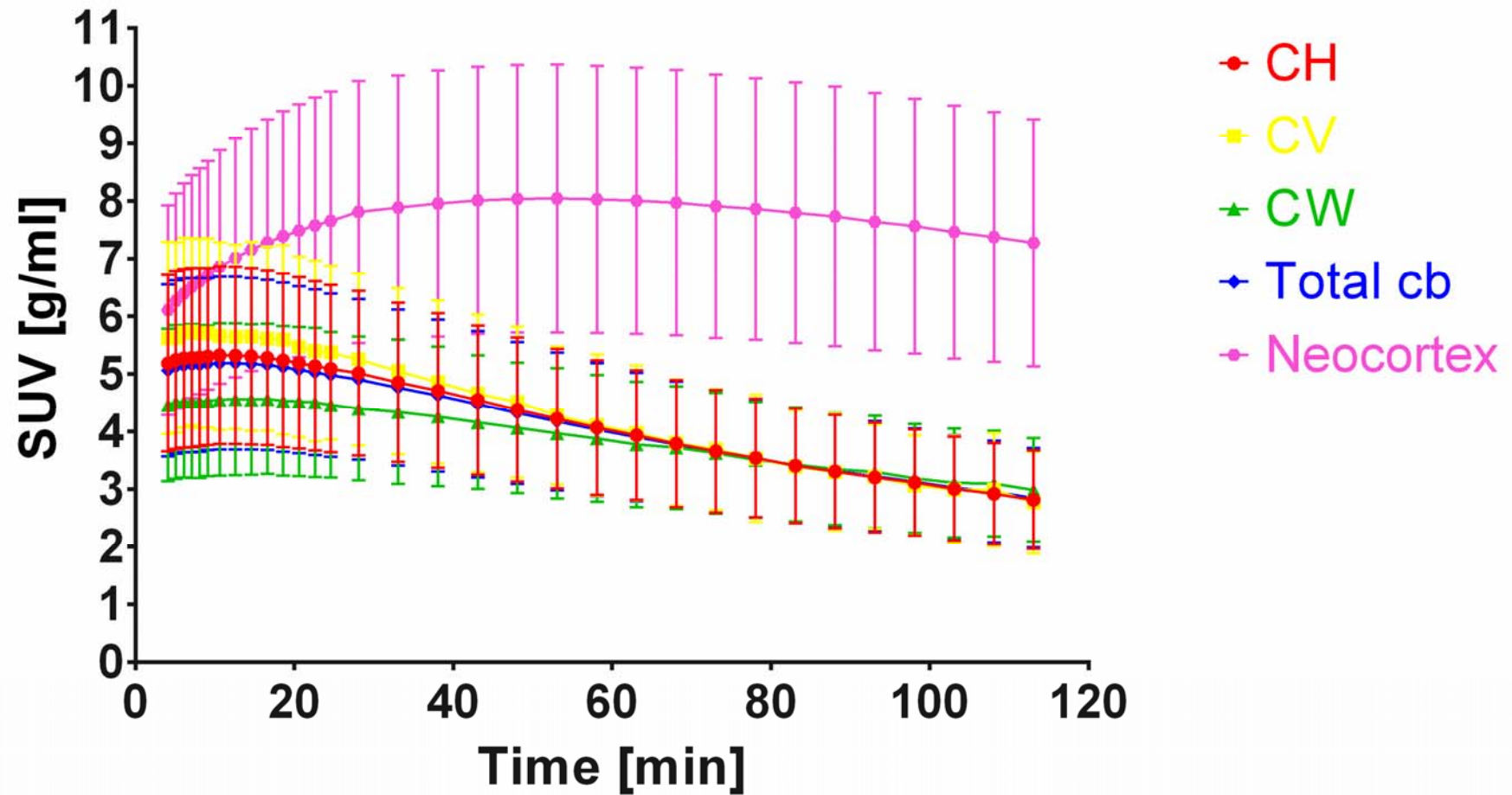
(a)

Mean SUV curves for [^{11}C]AZ10419369 (n=36)



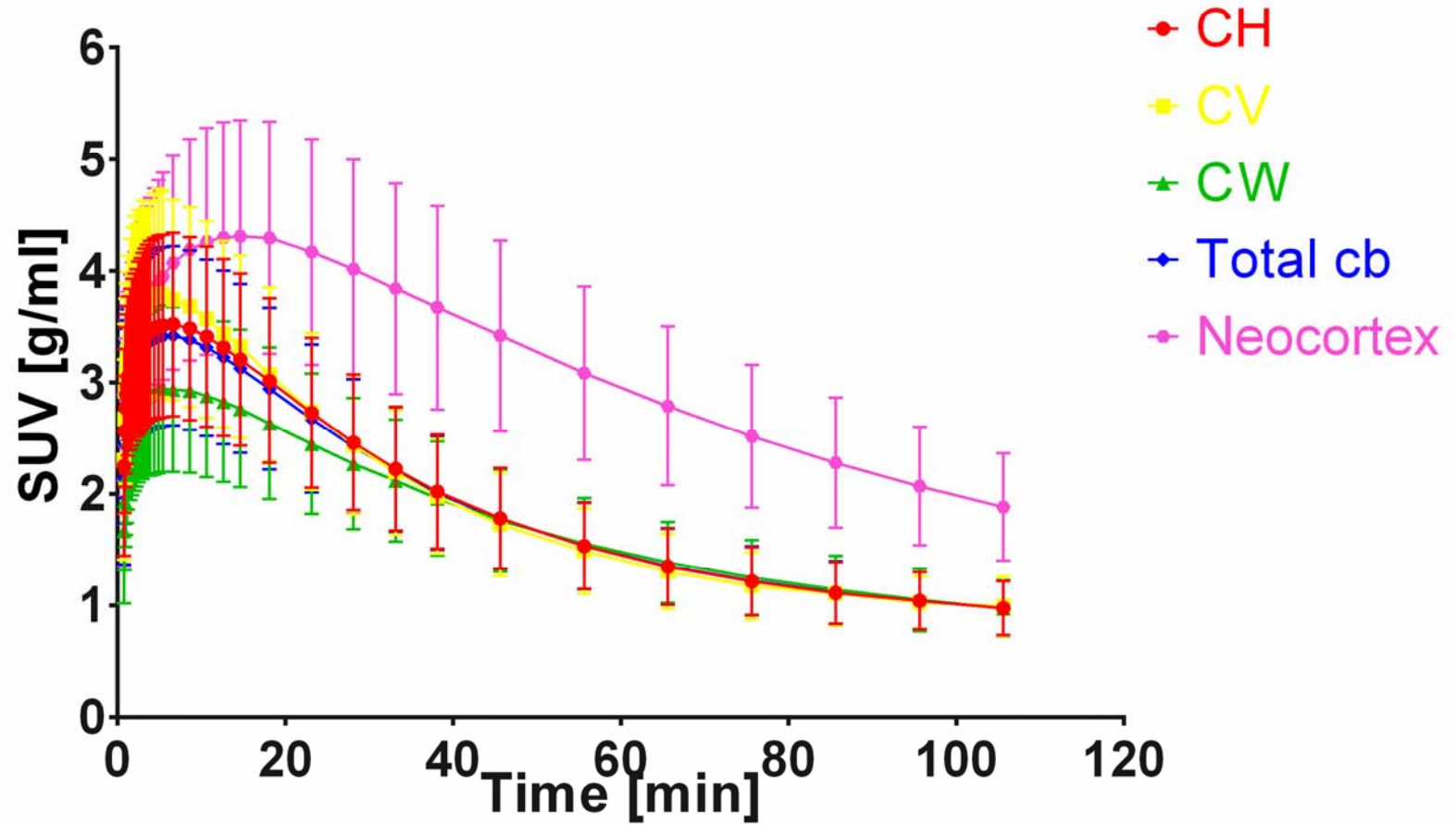
(b)

Mean SUV curves for [^{11}C]Cimbi-36 (n=29)



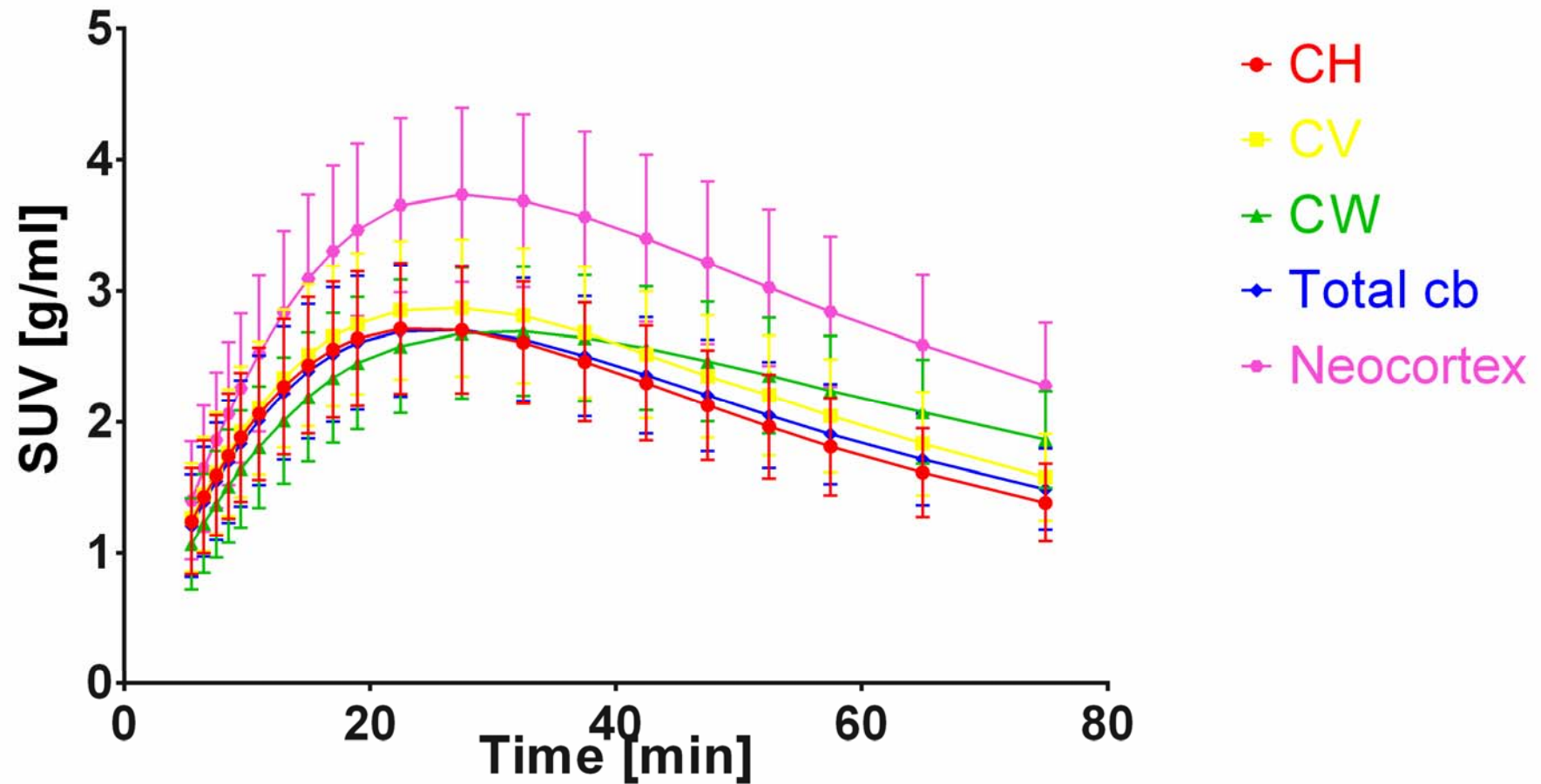
(c)

Mean SUV curves for [^{11}C]SB207145 (n=59)



(d)

Mean SUV curves for [^{11}C]DASB (n=100)



(e)

Figure 3. Population mean \pm standard deviation SUV curves for (a) [^{11}C]CUMI-101 (n=8), (b) [^{11}C]AZ10419369 (n=36), (c) [^{11}C]Cimbi-36 (n=29), (d) [^{11}C]SB207145 (n=59) and (e) [^{11}C]DASB (n=100).

References

1. Benjamini Y, Hochberg Y. Benjamini Y, Hochberg Y. Controlling the false discovery rate: a practical and powerful approach to multiple testing. *J R Stat Soc B* 1995; 57: 289–300.
2. Ettrup A, da Cunha-Bang S, McMahon B, et al. Serotonin 2A receptor agonist binding in the human brain with [¹¹C]Cimbi-36. *J Cereb Blood Flow Metab* 2014; 34: 1188–96.